



HAL
open science

X-ray absorption spectroscopy evidence of sulfur-bound cadmium in the Cd-hyperaccumulator *Solanum nigrum* and the non-accumulator *Solanum melongena*

Marie-Laure Pons, Blanche Collin, Emmanuel Doelsch, Perrine Chaurand, Till Fehlaue, Clément Levard, Catherine Keller, Jérôme Rose

► To cite this version:

Marie-Laure Pons, Blanche Collin, Emmanuel Doelsch, Perrine Chaurand, Till Fehlaue, et al.. X-ray absorption spectroscopy evidence of sulfur-bound cadmium in the Cd-hyperaccumulator *Solanum nigrum* and the non-accumulator *Solanum melongena*. *Environmental Pollution*, 2021, 279, pp.116897. 10.1016/j.envpol.2021.116897 . hal-03184158

HAL Id: hal-03184158

<https://hal.science/hal-03184158v1>

Submitted on 29 Mar 2021

HAL is a multi-disciplinary open access archive for the deposit and dissemination of scientific research documents, whether they are published or not. The documents may come from teaching and research institutions in France or abroad, or from public or private research centers.

L'archive ouverte pluridisciplinaire **HAL**, est destinée au dépôt et à la diffusion de documents scientifiques de niveau recherche, publiés ou non, émanant des établissements d'enseignement et de recherche français ou étrangers, des laboratoires publics ou privés.

Journal Pre-proof

X-ray absorption spectroscopy evidence of sulfur-bound Cadmium in the Cd-hyperaccumulator *Solanum nigrum* and the non-accumulator *Solanum melongena*

Marie-Laure Pons, Blanche Collin, Emmanuel Doelsch, Perrine Chaurand, Till Fehlaue, Clément Levard, Catherine Keller, Jérôme Rose



PII: S0269-7491(21)00479-6

DOI: <https://doi.org/10.1016/j.envpol.2021.116897>

Reference: ENPO 116897

To appear in: *Environmental Pollution*

Received Date: 3 December 2020

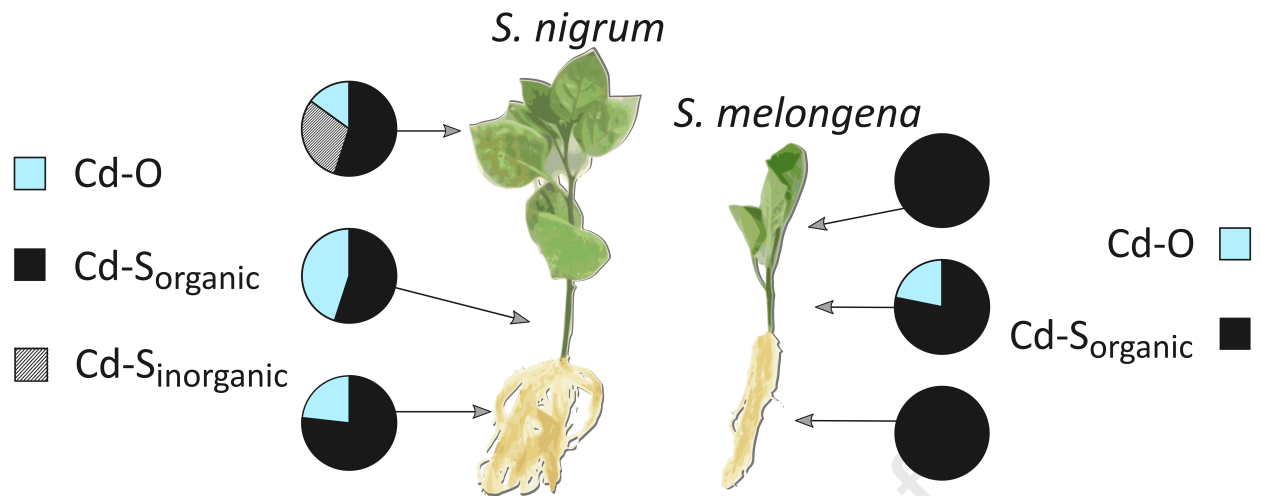
Revised Date: 24 February 2021

Accepted Date: 2 March 2021

Please cite this article as: Pons, M.-L., Collin, B., Doelsch, E., Chaurand, P., Fehlaue, T., Levard, C., Keller, C., Rose, J., X-ray absorption spectroscopy evidence of sulfur-bound Cadmium in the Cd-hyperaccumulator *Solanum nigrum* and the non-accumulator *Solanum melongena*, *Environmental Pollution*, <https://doi.org/10.1016/j.envpol.2021.116897>.

This is a PDF file of an article that has undergone enhancements after acceptance, such as the addition of a cover page and metadata, and formatting for readability, but it is not yet the definitive version of record. This version will undergo additional copyediting, typesetting and review before it is published in its final form, but we are providing this version to give early visibility of the article. Please note that, during the production process, errors may be discovered which could affect the content, and all legal disclaimers that apply to the journal pertain.

© 2021 Elsevier Ltd. All rights reserved.



1 **X-ray absorption spectroscopy evidence of sulfur-bound Cadmium**
2 **in the Cd-hyperaccumulator *Solanum nigrum* and the non-**
3 **accumulator *Solanum melongena***

4
5 Marie-Laure Pons^{a1*}, Blanche Collin^a, Emmanuel Doelsch^b, Perrine Chaurand^a, Till
6 Fehlauer^a, Clément Levard^a, Catherine Keller^a and Jérôme Rose^a

7 a: Aix Marseille Univ, CNRS, IRD, INRAE, Coll France, CEREGE UMR 7330, Aix en
8 Provence, France

9 b: CIRAD, UPR Recyclage et risque, F-34398 Montpellier, France Recyclage et Risque,
10 Univ Montpellier, CIRAD, Montpellier, France

11
12 **Corresponding author.** Marie-Laure Pons* pons@cerege.fr

13
14
15

¹ Permanent email address: dr.marie.laure.pons@gmail.com

Abstract

16 **Abstract**
17 It has been proposed that non-protein thiols and organic acids play a major role in
18 cadmium phytoavailability and distribution in plants. In the Cd-hyperaccumulator *Solanum*
19 *nigrum* and non-accumulator *Solanum melongena*, the role of these organic ligands in the
20 accumulation and detoxification mechanisms of Cd are debated. In this study, we used X-
21 ray absorption spectroscopy to investigate Cd speciation in these plants (roots, stem,
22 leaves) and in the soils used for their culture to unravel the plants responses to Cd
23 exposure. The results show that Cd in the 100 mg.kg⁻¹ Cd-doped clayey loam soil is
24 sorbed onto iron oxyhydroxides. In both *S. nigrum* and *S. melongena*, Cd in roots and
25 fresh leaves is mainly bound to thiol ligands, with a small contribution of inorganic S
26 ligands in *S. nigrum* leaves. We interpret the Cd binding to sulfur ligands as detoxification
27 mechanisms, possibly involving the sequestration of Cd complexed with glutathione or
28 phytochelatins in the plant vacuoles. In the stems, results show an increase binding of Cd
29 to -O ligands (>50% for *S. nigrum*). We suggest that Cd is partly complexed by organic
30 acids for transportation in the sap.

31

Capsule

32 **Capsule**
33 Cadmium speciation in Solanaceae was investigated using X-ray absorption spectroscopy.
34 Results showed evidence of Cd detoxification through Cd binding with thiols and inorganic
35 sulfur.

36

Keywords

37 **Keywords**
38 Cadmium, Speciation, Toxicity, Solanaceae, X-ray absorption spectroscopy.

39

40

41

1. Introduction

Cadmium contamination in agricultural soils has raised worldwide concerns, as its release in the environment dramatically increased in the past decades due to various anthropogenic activities such as smelting, combustion of coal or inorganic phosphate fertilization (Cai et al., 2003; Cullen and Maldonado, 2013; Dharma-wardana, 2018; Zhou and Song, 2004). Cadmium is toxic toward almost all forms of life, even at low concentrations (Cullen and Maldonado, 2013; Das et al., 1997). With relatively high mobility in the soil/plant system, Cd easily enters the food chain and poses human health threats (Cullen and Maldonado, 2013; Das et al., 1997). Previous studies have demonstrated that the mobility and bioavailability of Cd in the soil/plant system – thus its toxicity in this system – depends ultimately on its chemical speciation (Cullen and Maldonado, 2013).

The development of direct, experimental characterization of trace elements speciation by X-ray absorption spectroscopy (XAS) has brought key information on trace metal behavior in the critical zone (Collin et al., 2014; Doelsch et al., 2006; Huguet et al., 2012; Isaure et al., 2015; Sarret, 2002; Sarret et al., 2013). However, applying this methodology to the determination of Cd speciation in biological samples remains challenging as in most plants, Cd concentration (e.g. 0.01-1 mg.kg⁻¹ dry weight) lies below the technical detection limit of most X-ray absorption synchrotron beamlines. That is why, to date, Cd speciation determination has mainly been carried out on Cd-hyperaccumulating and/or Cd-tolerant plant systems (Huguet et al., 2015, 2012; Isaure et al., 2015). These pioneering studies demonstrated a change in Cd speciation upon Cd uptake through the roots, and during Cd translocation and storage in the leaves, and the involvement of thiols, organic acids and phosphate ligands in response to Cd exposure (Huguet et al., 2012; Isaure et al., 2015, 2006). Recent progress in XAS spectroscopy triggered by the development of highly sensitive fluorescence detectors have opened the field of Cd speciation determination in

68 plants with very low Cd concentrations such as cacao (Vanderschueren et al., 2020) or
69 rice (Wiggenhauser et al., 2020) and have identified new Cd ligands like histidine
70 (Vanderschueren et al., 2020), proving that XAS techniques still have a lot to offer to better
71 characterize Cd behavior in the soil/plant system.

72 Here, we investigated Cd speciation in plants from the solanum family, Cd-
73 hyperaccumulator *Solanum nigrum* (*S. nigrum*; *black nightshade*) and non-tolerant (Sun et
74 al., 2006) *Solanum melongena* (*S. melongena*; *eggplant*). Among the solanum family,
75 several species are cultivated worldwide as food products – e.g. tomatoes, potatoes, bell
76 peppers, eggplants, and have shown a tendency to Cd accumulation (e.g. eggplants, Sun
77 et al., 2006; tomatoes, Hasan et al., 2019). Deciphering their responses to Cd exposure is
78 of prime interest for food safety reasons. The mechanisms governing Cd distribution in
79 these plants are still debated. Sun et al., (2006) study proposes that organic acids play a
80 major role in solanum species behavior toward Cd (Li et al., 2020; Sun et al., 2006), as
81 they found increasing carboxylic acid contents in *S. nigrum* and *S. melongena* leaves
82 when exposed to high level of Cd. By chemical titration, they reported organic acid over Cd
83 ratios of ~ 1000 (Sun et al., 2006) and suggested that Cd accumulation and detoxification
84 in these plants is regulated by complexation with organic acids alone. The involvement of
85 organic acids in the handling of Cd has been invoked in other Solanaceae, such as tomato
86 (Bao et al., 2011b). However, other studies reported, by chemical extraction and titration,
87 an increase of thiol compounds – cysteine, glutathione and phytochelatins – in solanum
88 plants exposed to Cd (Chamseddine et al., 2008; Gao et al., 2010; Hasan et al., 2019,
89 2015), including *S. nigrum* (Gao et al., 2010). In this context, this study aims at deciphering
90 the fate of Cd in the solanum plants at the molecular level by performing, for the first time,
91 Cd speciation characterization in Solanaceae using XAS spectroscopy.

92

93

94

95 **2. Materials and methods**

96

97 **2.1. Plant and soil material**

98 500 seeds of *Solanum nigrum* – reference ‘blackberry nightshade’ – and *Solanum*
99 *melongena* – reference ‘black beauty eggplant’ were purchased at a local gardening store.

100 The soil used in this study is a clayey loam soil (LUFA Speyer standard 2.4, Table S1).

101 The soil was freshly field collected in a meadow with apple trees, then sieved at 2 mm and

102 analyzed before shipment. Upon reception at the CEREGE, the soil was incubated with

103 100 mg.kg^{-1} Cd as dissolved cadmium nitrate tetrahydrate (98%, Sigma-Aldrich). Such

104 elevated Cd concentration, albeit ~20 times higher than reported values for Cd agricultural

105 soils from the industrialized Chenzhou region in China (Robson et al., 2014; Wang et al.,

106 2019; Zhai et al., 2008) and ~200 times higher than the average Cd geochemical

107 background in French soils (Baize, 1997), was chosen to ensure sufficient uptake of Cd by

108 the plants prior to XAS analyses. We aimed at Cd content of $>50 \text{ }\mu\text{g.g}^{-1}$ dry weight in the

109 plant parts, which was previously reported in *S. nigrum* and *S. melongena* grown on a 100

110 mg.kg^{-1} Cd-doped soil (Sun et al., 2006). The Cd-doped soil was brought to 70% of its

111 maximum water holding capacity using deionized water, thoroughly mixed then stored for

112 4 weeks in a growth chamber with controlled humidity, at a temperature of 24°C. A control

113 soil was also prepared, without Cd, but with the same amount of nitrate as dissolved

114 NaNO_3 , following the same procedure.

115

116 **2.2. Plant cultures**

117 *Solanum nigrum* and *S. melongena* seeds were placed on some clean KimTech™ wipes

118 soaked with deionized water, in Plexiglas boxes, at 28°C for 14 days, for germination.

119 Plastic gardening pots of 14 cm diameter were prepared with 2 cm of sand at the bottom

120 and ~500 g of incubated Cd-doped or control soil in each pot. Two-week-old seedlings of
121 *S. nigrum* and *S. melongena* with shoots of about 2 cm were then transplanted into the
122 pots (2 seedlings per pot). Six pots per plant type were prepared for the Cd-doped soil and
123 for the control soil. Plants were cultivated in a controlled growth chamber with fixed
124 temperature of 24°C, controlled humidity, and photoperiod (light: 6 am – 9 pm). Each pot
125 was automatically watered individually with deionized water, twice a day (at 9 am and 5
126 pm), to maintain the soil at 70% of its maximum water holding capacity. No fertilizer was
127 added. The plants were harvested after a growth period of 14 weeks. For each plant type
128 and soil treatment, four replicates were used for total Cd content analyses and 3 replicates
129 were prepared for XAS measurements, following two protocols detailed in the next two
130 paragraphs.

131

132 **2.3. Analysis of total Cd content in the plant parts (exposed and control samples)**

133 After harvest, roots and aerial parts have been separated at the collar level and cleaned
134 with ultrapure water (18.2 MΩ·cm). Roots received additional cleaning by gentle brushing
135 and vortexing in water. Fresh leaves and stems were separated. Plant samples were dried
136 in an oven set at 40°C during 48h. Roots, stems and fresh leaves were weighed before
137 (fresh weight) and after drying (dry weight; Tables S6 and S7). Plant samples (roots, fresh
138 leaves, stems) were ground for 2min at 20hz with a Retsch® Mixer Mill MM 400 to obtain a
139 fine powder. 100 to 300 mg of each plant sample was then digested in a mixture of nitric
140 acid, hydrochloric acid and peroxide using a microwave (MLS turboWAVE®). Total
141 cadmium analyses were performed on the Q-ICPMS (quadrupole-inductively coupled
142 plasma mass spectrometer, Perkin Elmer Nexlon 300X).

143

144 **2.4. Synchrotron X-ray absorption measurements**

145 **Plants and soils preparation for XAS measurements.** After Cd incubation, and prior to
146 the pot experiments, ~50 g of soil was frozen in a -80°C freezer to avoid changes in
147 speciation. This initial soil will be referred as 'pre-culture soil t_0 '. After 14 weeks of pot
148 experiments, *S. nigrum* and *S. melongena* samples were carefully harvested and cleaned.
149 Roots received additional cleaning by gentle brushing and vortexing in water. Special
150 attention was paid to ensure that no soil residue would remain on any parts of the plants,
151 especially on the roots of both *S. nigrum* and *S. melongena* and on the dead leaves of *S.*
152 *melongena*, to prevent soil Cd contamination of the plant tissues. For XAS measurements,
153 *S. nigrum* plants were cut and divided into: roots, top fresh leaves, bottom fresh leaves,
154 and stem. *Solanum melongena* plants were cut and divided into: roots, fresh leaves, stem
155 and dead leaves (detached from the plant). All plant parts were weighed then directly
156 frozen in liquid nitrogen and stored in a -80°C freezer, to prevent any speciation change
157 before the synchrotron measurements. All further preparation steps were performed
158 frozen, using liquid nitrogen. Cryogenic grinding was performed on all plant and soil
159 samples using zirconium oxide beads in 2 mL Eppendorf tubes with a Retsch® Mixer Mill
160 MM 400. 7 mm diameter pellets were then prepared using a hand press with dies cooled in
161 liquid nitrogen. Samples were transported to the Diamond Light Source and to Soleil
162 Synchrotron on dry ice.

163

164 **Cd reference compounds.** A large database of Cd-containing reference compounds was
165 analyzed for X-ray Absorption Near Edge Structure (XANES) and Extended X-ray
166 Absorption Fine Structure (EXAFS) to allow the interpretation of XAS spectra obtained on
167 the soil and plant natural samples (Huguet et al., 2015, 2012; Isaure et al., 2015;
168 Vanderschueren et al., 2020). Some of these Cd reference materials were purchased
169 chemicals, the others were prepared at the laboratory. Commercial Cd minerals included
170 CdS, Cd(OH)₂, CdO, CdCl₂, CdPO₄, CdCO₃ and CdSO₄. A solution of aqueous Cd²⁺

171 $(\text{Cd}(\text{H}_2\text{O})_6^{2+})$ reference was prepared by dissolving commercial $\text{Cd}(\text{NO}_3)_2(\text{H}_2\text{O})_4$ in Milli-Q
172 water. A library of Cd-organic complexes, composed of several Cd bound to organic acids
173 relevant to the solanum species (Sun et al., 2006) – Cd-acetate, Cd-malate, Cd-citrate,
174 Cd-tartrate, Cd-phytate – as well as thiol Cd compounds – Cd-glutathione, Cd-cysteine –
175 and amino acid Cd-histidine, were synthesized in the laboratory (Supplementary Material
176 Part 1). To better constrain Cd speciation in the soil, we also analyzed a synthetic Cd-
177 sorbed goethite (Hammer et al., 2006) and a naturally Cd-rich calcite collected at Dornach
178 (NW Switzerland). The compounds CdS, $\text{Cd}(\text{OH})_2$, CdO and CdSO_4 were prepared as
179 pressed pellets diluted with PVP, while all other references were prepared as liquid
180 solutions. Prior to XAS measurements, pellets or liquid references were frozen in liquid
181 nitrogen. Spectra for all Cd-containing pellet references and Cd glutathione, Cd
182 phosphate, Cd acetate and $\text{Cd}(\text{H}_2\text{O})_6^{2+}$ solutions were recorded at Cd K-edge in
183 transmission mode. Other liquid references were measured at Cd K-edge in fluorescence
184 mode. The Cd K-edge EXAFS spectra of all Cd reference compounds and their Fourier
185 transforms are presented in Figure S2. The Cd K-edge XANES spectra of all Cd reference
186 compounds are presented in Figure S3.

187

188 **Cd K-edge XANES and EXAFS Spectroscopy.** Cd K-edge ($E_0=26711$ eV) XANES and
189 EXAFS experiments were performed during two synchrotron facility sessions carried out at
190 the Diamond Light Source (Didcot, United Kingdom) and at the SOLEIL synchrotron facility
191 (Saint-Aubin, France). At the Diamond Light Source, the experiments were performed on
192 the B18 core XAS beamline (for more information on the beamline, see the supplementary
193 materials, part 2), which is equipped with a Si (311) monochromator for measurements at
194 high energy (>20 keV). The storage ring was operated at 3 GeV with a ring current of 300
195 mA. Samples were measured using a 35-element germanium Solid State Detector (SSD)
196 in fluorescence detection mode. X-ray absorption spectra were scanned from 26523 eV to

197 27093 eV for the diluted samples and from 26523 eV to 27711 eV for the references in
198 quick EXAFS mode (~ 4 min per spectrum). For each sample, 100 to 180 spectra were
199 acquired, aligned, and merged. The energy calibration was performed using a Cd foil
200 sheet. The beam spot size was set to 1.5 x 1.5 mm. To avoid Cd speciation change during
201 measurements, the sample pellets and liquid references were measured using a liquid
202 nitrogen Oxford Optistat cryostat set at 93K. At the Soleil Synchrotron, the experiments
203 were performed on the SAMBA beamline (for more information on the beamline, see the
204 supplementary materials, part 2), which is equipped with a Si (220) monochromator for
205 measurements at high energy (>20 keV). The storage ring was operated at 2.75 GeV with
206 a ring current of 500 mA. Samples were measured using a 35-element germanium SSD in
207 fluorescence detection mode. X-ray absorption spectra were scanned from 26523 eV to
208 27093 eV for the diluted samples and from 26523 eV to 27711 eV for the references in
209 quick EXAFS mode (~ 3 min per spectrum). For each sample, 50 to 110 spectra were
210 acquired, aligned, and merged. The energy calibration was performed using a Cd foil
211 sheet. The beam spot size was set to 2 x 0.5 mm. All samples and references were
212 measured using a liquid nitrogen cryostat set at 80K.

213 For all samples, the extracted EXAFS spectra were k^2 weighted (with k : wave vector) to
214 enhance the high- k region. Data treatment was performed using the ATHENA (Ravel and
215 Newville, 2005), ARTEMIS (Ravel and Newville, 2005) and FASTOSH (Landrot, 2018)
216 softwares. Fourier transforms were performed of the k range from 2 to 9 \AA^{-1} to R space
217 using a Hanning apodization window. The structural and chemical parameters of the
218 references (Table S3) and of the soil samples (Table S10) were modelled by shell-by-shell
219 fitting using the ARTEMIS software. Shell-fitting analysis of the k^2 -weighted EXAFS
220 spectra was performed in R -space. Theoretical EXAFS phase-shift and amplitude
221 functions for the paths were calculated using FEFF (Rehr et al., 2010). Principal
222 component analyses (PCA) were performed on the soil samples and on the plant samples

223 to determine the number of references needed to explain our datasets. PCA were the
224 FASTOSH software (Landrot, 2018). Target transform were performed on every single Cd
225 reference compound to assess whether they constitute good candidates to explain Cd
226 speciation in our soil/plant system (Wasserman, 1997; Wasserman et al., 1999). The best
227 linear combination fitting (LCF) of our samples EXAFS spectra were determined using the
228 LCF fitting module of the FASTOSH software over the k range 2 to 9 Å⁻¹ with a fixed E₀
229 value of 26710.4 eV. Residual factor of LCF was calculated using the following equation:

$$230 \quad R = \frac{\sum(k^2 \chi(k)_{exp} - k^2 \chi(k)_{fit})^2}{\sum(k^2 \chi(k)_{exp})^2}$$

231 At each step of the fitting, an additional reference spectrum was added if the two following
232 conditions were true: the R factor decreased by 20% or more and the additional reference
233 had a contribution equal to or higher than 10% among Cd-species. For the same number
234 of references, two different LCF fittings are considered undistinguishable if their R factor is
235 comprised within 20%. The uncertainty of this LCF method was estimated at +/-15%
236 (Doelsch et al., 2006; Le Bars et al., 2018). PCA, target transforms and LCF fittings are
237 further discussed in the results part and in the supplementary material (Part 3).

238

239 **3. Results and discussion**

240

241 **3.1. Plant Cd content and aspect**

242 *Solanum nigrum* has been identified as a potential Cd-hyperaccumulator plant (Sun et al.,
243 2006; Wei et al., 2005). The definition of hyperaccumulation depends on the considered
244 metal. For Cd, several studies have proposed to define Cd hyperaccumulation ability as
245 the accumulation of Cd in the stems or leaves of the plant exceeding the threshold of 100
246 µg.g⁻¹, dry weight (Baker et al., 2000; Huguet et al., 2015; Isaure et al., 2015; Lu et al.,
247 2013; Sun et al., 2011, 2006; Uraguchi et al., 2006; Wei et al., 2005). In our experiments,

248 *S. nigrum* leaves show average values of $126.5 \pm 12 \mu\text{g.g}^{-1}$ Cd in leaves (DW, Table 1).
249 60% of *S. nigrum* total Cd content is located in its shoots (6% in the stem, 54% in the
250 leaves, Table 1). In Sun et al., 2006, *S. melongena* has been described as 'less tolerant'
251 towards Cd than *S.*

252

253 *nigrum*. For *S. melongena* plants grown on a 100 mg.kg^{-1} Cd doped soil, they report Cd
254 concentrations of $64 \mu\text{g.g}^{-1}$ (DW) in leaves and $189 \mu\text{g.g}^{-1}$ (DW) in roots. Our results are
255 consistent with these values, with Cd concentrations of $59 \mu\text{g.g}^{-1}$ (DW) in leaves and 244
256 $\mu\text{g.g}^{-1}$ (DW) in roots (Table 1). While *S. melongena* does not fit the definition of Cd-
257 hyperaccumulation, *S. melongena* does accumulate a significant amount of Cd when
258 exposed to this metal. Our results show that *S. nigrum* display enhanced capacity to
259 accumulate Cd in its aerial parts (60% total Cd in stem + leaves) compared to *S.*
260 *melongena* (41%, Table 1), with a slightly higher roots to aerial parts Cd translocation
261 factor (0.31 for *S. nigrum* and 0.24 for *S. melongena*; a Student t-test identifies the two
262 groups as distinct at a 93.7% confidence interval; Table S7).

263 *Solanum nigrum* plants grown on the Cd-doped soil show signs of leaf chlorosis in the
264 older, bottom leaves (Figure S4), as well as significantly (Student t-test, 95% C.I.) lower
265 roots, stem and leaves biomass compared to plants grown on the control soil (Figure 1,
266 Figure S5 and Table S6 and S7). *Solanum melongena* plants grown on 100 mg.kg^{-1} Cd-
267 doped soil have roots that display more friable texture than that of the control plants. No *S.*
268 *melongena* plants from the Cd doped experiment reached a stage where more than two
269 leaves were present at the same time, while *S. nigrum* plants reached a more mature
270 stage (up to 10 leaves). *Solanum melongena* plants exposed to Cd also show significantly
271 (Student t-test, 95% C.I.) lower roots biomass, and a tendency to lower stem and leaves
272 biomass compared to the control plants (Figure 1 and Table S6 and S7). For both *S.*
273 *nigrum* and *S. melongena*, all of the above constitute well-described consequences of

274 exposure to high levels of Cd (Das et al., 1997; Maqbool et al., 2019; Prasad, 1995;
275 Rizwan et al., 2012).

276

277

278

279 Table 1: Cd average concentrations, dry weights, and total Cd contents measured in *S. nigrum* and *S. melongena* grown
280 on 100 mg.kg⁻¹ Cd doped clayey loam soil.

281

plant type	soil Cd concentration	Plant Part	Cd ($\mu\text{g}\cdot\text{g}^{-1}$)		DW (mg)		Cd (μg)		Cd (%)	
			measured on dry sample (± 1 s.d.)	n	Dry weight (± 1 s.d.)	n	Average total Cd content	Average total Cd content		
<i>S. melongena</i>	100 mg.kg ⁻¹	Roots	243.8 \pm 9	4	39.8 \pm 10	4	9.7	59		
		Stem	58.5 \pm 10	4	28.9 \pm 4	4	1.7	10		
		Fresh leaves	58.8 \pm 10	4	87.1 \pm 38	4	5.2	31		
<i>S. nigrum</i>	100 mg.kg ⁻¹	Roots	376.8 \pm 87	4	33.6 \pm 17	4	12.5	40		
		Stem	43.8 \pm 6	4	41.4 \pm 26	4	1.8	6		
		Fresh leaves	126.5 \pm 12	4	130.8 \pm 40	4	16.7	54		

282

283

284 3.2. No change in soil Cd speciation upon plant culture

285 Cadmium speciation in the 100 mg.kg⁻¹ Cd doped soil before and after culture of both
286 *Solanum nigrum* and *S. melongena* was assessed by EXAFS spectroscopy. Principal
287 component analysis (PCA) performed on EXAFS spectra of six soil samples identified up
288 to two components (Supplementary material Part 3), meaning one to two Cd reference
289 compounds are needed to reconstruct soil samples EXAFS spectra through linear
290 combination fitting (LCF). XAS spectra of pre- and post-culture soils for both *S. nigrum* and
291 *S. melongena* are visually almost identical (Figure S6). They are also very similar to the
292 spectrum of the Cd-sorbed artificial goethite we measured (Figure S6). Sorption of Cd onto
293 oxides and hydroxides in soils is a known mechanism that has been documented in
294 several studies, for example Cd sorption on manganese oxyhydroxides (Chen et al., 2019;

295 Kubier et al., 2019; Lin et al., 2016; Wasylenki et al., 2014) or iron oxyhydroxides,
296 including goethite (Barrow et al., 1989; Bruemmer et al., 1988; Gerth et al., 1993; Gerth
297 and Bruemmer, 1983). However, due to the low amount of Cd in the goethite reference
298 ($\sim 50 \text{ mg.kg}^{-1} \text{ Cd}$), the Cd-sorbed goethite EXAFS spectrum presents significant noise in
299 the high k region. For these reasons, we chose to use the XANES part of our soil samples
300 spectrum (from -30 eV to +100 eV) to perform linear combination fittings. Figure 2 shows
301 our soil samples XANES spectra and their best fit, along with Cd-sorbed goethite, Cd-
302 phytate and Cd-organic acids reference spectra. In the pre-culture, $100 \text{ mg.kg}^{-1} \text{ Cd}$ -doped
303 soil, the spectrum was best reconstructed with 100% Cd-sorbed goethite (Figure 3;
304 Supplementary Table S9). Post-culture *S. nigrum* soil XANES LCF fit gives the same
305 result: 100 % Cd sorbed onto goethite. For *S. melongena* post-culture soil, our fitting
306 method suggests a contribution of Cd bound to organic acids, with the best LCF fits giving
307 85% Cd sorbed to goethite and 15% Cd bound to acetate. Our LCF method also gave
308 acceptable results for citrate, malate and tartrate as oxygen ligand candidates. The
309 secretion of organic acids in roots exudates is a well-documented phenomenon (Adeleke
310 et al., 2017; Bao et al., 2011b; Han et al., 2006; Loganathan et al., 2012). In various plant
311 families, including solanum plants, the root exudation of organic acids enhances the
312 bioavailability of nutrient metals such as zinc or iron in soils (Bao et al., 2011a;
313 Samardjieva et al., 2015). Cadmium is a non-essential cation with similar properties as
314 zinc. The release of organic acids by *S. melongena* roots in the soil might consequently
315 cause partial Cd desorption from oxyhydroxides and enhance Cd phytoavailability.
316 Changes in soil Cd speciation from Cd mineral species to Cd bound to organic acids after
317 plant culture has been previously identified by Huguet et al (Huguet et al., 2015). Overall,
318 considering our LCF method gives an uncertainty of $\pm 15\%$ on the percentage of Cd
319 species, our results for pre- and post-culture soils, regardless of the plant type, are quite
320 similar. This is consistent with the structural and chemical parameters we obtained by

321 performing a first shell fit of our soil samples Cd k-edge EXAFS spectra using the
322 ARTEMIS software (Ravel and Newville, 2005). All three samples show the same Cd
323 coordination to O atoms ($N \sim 5.6$) with Cd-O bond length of 2.26 Å (see Supplementary
324 Table S10), which is also very close to the structural parameters modelled for the Cd
325 sorbed goethite reference (backscatterer in the first coordination sphere: O; $N = 5.7$, Cd-O
326 $R = 2.25$ Å). We interpret this overall lack of differences in Cd speciation in soil before and
327 after culture as the expression of a mass balance effect. The total Cd content in *S.*
328 *melongena* and *S. nigrum* is ~ 30 µg (Table 1). Considering two plants per pot, the plants
329 have taken up 60 µg of Cd per pot, which represents 0.12% of the initial Cd content.
330 Despite the roots of both plants having colonized the whole pot, the bulk 500 g, 100 mg.kg⁻¹
331 ¹¹¹Cd-doped soil is not significantly affected by the plants.

332

333

334 3.3. Cd speciation in *S. nigrum* and *S. melongena*

335 Cd k-edge EXAFS spectra of plant parts and corresponding Fourier transforms are
336 presented in figure 4. Linear combination fitting (LCF) of *S. nigrum* and *S. melongena* plant
337 parts EXAFS spectra (from $k=2$ to $k=9$) were performed using the EXAFS spectra of all of
338 the Cd reference compounds measured in this study. The best linear combination fittings
339 of samples EXAFS spectra and associated Fourier transforms are also plotted in Figure 4
340 (for LCF numerical result, see Table S11). In our plant samples, the fitting of EXAFS
341 spectra allowed us to identify the first neighbor of Cd as oxygen or sulfur. As detailed in
342 the following paragraphs, potential -O ligands included organic acids, histidine, phytate or
343 $\text{Cd}(\text{H}_2\text{O})_6^{2+}$. Potential -S ligands included binding to mineral sulfur (CdS) and organic sulfur
344 as glutathione or cysteine. Obtained proportion of Cd-O and Cd-S species for best EXAFS
345 LCF fits are displayed in Figure 5. Cd k-edge XANES spectra of the plant samples are
346 presented in Figure S7. Linear combination fitting of *S. nigrum* and *S. melongena* plant

347 parts XANES spectra (from 26680 to 26810 eV) were performed using the XANES spectra
348 of all of the Cd reference compounds measured in this study (displayed in Figure S3). The
349 best linear combination fittings of samples XANES spectra are also plotted in Figure S7
350 (for LCF numerical result, see Table S11). Obtained proportion of Cd-O and Cd-S species
351 for best XANES LCF fits are displayed in Figure S8, alongside best EXAFS LCF fits for
352 comparison. As demonstrated by Figure S8 and LCF results in Table S11, both EXAFS
353 and XANES analyses give the same results. For this reason, we chose to use the EXAFS
354 data analyses for the plant samples.

355

356 **A change of Cd speciation upon plant uptake in the roots.** Our results show that the
357 main first neighbor of Cd in both *S. nigrum* and *S. melongena* roots is sulfur (77% and
358 100% respectively, Figures 4 and 5). In *S. nigrum* roots, the remaining Cd is bound to
359 oxygen. All the acceptable linear combination fittings involve the Cd-glutathione model
360 compound, a thiol molecule, as the S-bearing ligand (Supplementary material Part 1). For
361 the oxygen counterpart in *S. nigrum*, while the best residue (R factor) was obtained with
362 Cd-tartrate, the LCF method could not distinguish between $\text{Cd}(\text{H}_2\text{O})_6^{2+}$, Cd-histidine, or
363 any of the Cd-organic acids analyzed (malate, tartrate, citrate, and acetate).

364 These results first demonstrate a major change of Cd speciation between the soil (Cd
365 sorbed to goethite) and the roots (Cd mainly bound to organic -S) for both solanum
366 species. From our results alone, it is unclear how the Cd sorbed to goethite in the soil
367 becomes available to the plants. Several studies suggest that plants can participate in the
368 release and dissolution of Cd sorbed onto oxyhydroxides, as root exudation of organic
369 acids – particularly tartrate and acetate – is involved in heavy metal uptake by roots (Bao
370 et al., 2011b; Fan et al., 1997; Sun et al., 2006). The Cd in *S. melongena* and *S. nigrum*
371 roots is then mainly complexed with thiol ligands (100% for *S. melongena* and 77% for *S.*
372 *nigrum*). In *S. melongena*, most of the Cd is located in the roots (Table 1), that show Cd

373 concentration of ~5 times that of the stem and fresh leaves (Table 1) and a roots to aerial
374 parts translocation factor of ~0.24. In non-accumulator plants, Cd binding to thiols and
375 vacuolar sequestration of these complexes has been previously described as a
376 detoxification mechanism (Cobbett, 2000; Marentes and Rauser, 2007; Mendoza-Cózatl et
377 al., 2008; Pál et al., 2018; Uraguchi and Fujiwara, 2012; Wawrzyński et al., 2006), with
378 possible storage of these complexes in the roots (Cao et al., 2018; Nocito et al., 2011;
379 Rauser, 2003; Salt et al., 2002, 1995; Ueno et al., 2010; Wiggerhauser et al., 2020). The
380 binding of Cd to non-chelating thiols such as glutathione and cysteine or to chelating thiols
381 such as phytochelatins in the roots could immobilize Cd and prevent its translocation to the
382 aerial parts of the plant (Cao et al., 2018; Nocito et al., 2011; Salt et al., 2002). In rice, a
383 recent XAS study by Wiggerhauser and collaborators (Wiggerhauser et al., 2020)
384 demonstrated that Cd in roots is 100% bound to S ligands, bringing new, direct evidence
385 of the role of Cd binding to S in Cd sequestration in roots and echoing our findings. We
386 therefore conclude that Cd bound to organic -S ligands in *S. melongena* roots constitutes a
387 storage form that limits Cd translocation to aerial parts and participates in its detoxification.
388 In the Cd-hyperaccumulator *S. nigrum*, most of the Cd is bound to S ligands (77%) and the
389 Cd translocation factor from roots to aerial parts is 0.31. Like *S. melongena*, we suggest
390 that Cd in roots is mainly immobilized and stored as Cd-thiol complexes. Such mechanism
391 has also been suggested in the Cd-hyperaccumulator *Brassica juncea* L. for which Cd
392 coordination with S was demonstrated using XAS spectroscopy (Salt et al., 1995). For the
393 remaining 23% of Cd bound to oxygen in *S. nigrum* roots, we considered two scenarios: (i)
394 this Cd-O fraction is also a storage form or (ii) it represents a transient fraction that could
395 be translocated to the aerial parts. (i) Storage of Cd as Cd-O has been previously reported
396 in Cd-hyperaccumulator plants. In the Cd-hyperaccumulator plant *Thlaspi praecox*, a
397 Brassicaceae that can accumulate very high amount of Cd in its shoot ($>7500 \mu\text{g.g}^{-1}$, DW,
398 Lombi et al., 2000; Vogel-Mikuš et al., 2006), Vogel-Mikuš and her collaborators performed

399 XAS measurements and reported that, of the $858 \mu\text{g.g}^{-1}$ (DW) Cd in *T. praecox* roots, 79%
400 was bound to -O ligands (as Cd-O-C), and the remaining 21% was bound to -S ligands (as
401 thiols, Vogel-Mikuš et al., 2010). They suggest that Cd is mainly bound to cell-wall -O
402 ligand components or stored in the vacuoles, complexed with organic acids. Organic acid
403 vacuolar sequestration of cadmium, albeit limited in the roots compared to the shoots, is a
404 well-described detoxification mechanism in Cd hyperaccumulator plants (Han et al., 2006;
405 Huguet et al., 2012; Isaure et al., 2015; Küpper et al., 2004; Lombi et al., 2000; Maqbool et
406 al., 2019; Sun et al., 2011; Vogel-Mikuš et al., 2010). We cannot rule out that such
407 mechanism takes place in *S. nigrum* roots and account for part of the Cd-O we reported.
408 (ii) However, given that Cd speciation in *S. nigrum* stem shows an increase in Cd binding
409 to O ligands (55%, Figure 5) for an amount of $\sim 3.3\%$ of the plant total Cd (Table 1), we
410 consider that the Cd bound to O in the roots ($\sim 9.2\%$ of the plant total Cd) could be a Cd
411 transient form for roots to aerial parts translocation. This Cd transport form hypothesis will
412 be further discussed in the next paragraph on Cd speciation in the stems.

413

414 **Cadmium transport forms in *S. nigrum* and *S. melongena* stems.** The linear
415 combination fittings of stem EXAFS spectra show contrasting results for *S. nigrum* and *S.*
416 *melongena*, as the main first neighbor of Cd for *S. nigrum* is O (55% O, 45 % S, Figure 5)
417 while it is S for *S. melongena* (78% S, 22% O, Figure 5). For *S. nigrum*, the best LCF
418 fittings involve non-protein thiol glutathione as the S-bearing ligand. For the O ligand in *S.*
419 *nigrum*, the best fit is obtained with acetate, but other organic acids malate, citrate, and
420 tartrate, as well as $\text{Cd}(\text{H}_2\text{O})_6^{2+}$, histidine, give acceptable results according to our LCF
421 method. As for *S. melongena*, all the best LCF give glutathione as the S bearing ligand,
422 and tartrate as the best O ligand. Other organic acids, $\text{Cd}(\text{H}_2\text{O})_6^{2+}$, histidine and phosphate
423 also give acceptable results.

424 *S. melongena* stem and fresh leaves display very similar cadmium concentrations (~58
425 $\mu\text{g}\cdot\text{g}^{-1}$ DW, Table 1), much lower than that of the roots (~250 $\mu\text{g}\cdot\text{g}^{-1}$ DW). Compared to *S.*
426 *nigrum*, for which fresh leaves Cd concentration is three times higher than in stem (~127
427 and ~44 $\mu\text{g}\cdot\text{g}^{-1}$ DW respectively, Table 1), our results point towards a more limited
428 translocation of Cd in *S. melongena* stem. Previous studies demonstrated – using XAS
429 spectroscopy (Salt et al., 2002, 1995) – or suggested (using chemical titration, Mendoza-
430 Cózatl et al., 2008) that Cd can be transported in the xylem sap bound to oxygen bearing
431 components. Our EXAFS measurements show that the binding of Cd to O ligands in *S.*
432 *melongena* is restricted to the stem, which we interpret as Cd transportation form in the
433 saps. In *S. nigrum*, Cd concentration and contents in the plant parts (Table 1) indicate a
434 more intense translocation of Cd from the roots to the leaves, where Cd is stored. As
435 mentioned earlier, the amount of Cd bound to oxygen ligands in the stem (55% of stem
436 Cd; ~3.3% of the plant total Cd) is close to that of the roots (~9.2% total Cd). This value is
437 also similar to the one in *S. nigrum* fresh top leaves (15% Cd-O in the leaves; 8.1% of the
438 plant total Cd, Figure 5). We interpret these results as an argument in favor of Cd-O being
439 the translocation form for Cd in *S. nigrum*.

440 Like *S. melongena*, we propose that the prevalence of O ligands in the stem of *S. nigrum*
441 is to be attributed to the transport form of Cd in the xylem sap. Our results suggest that Cd
442 is transported bound to O ligands, unlike what was observed in *Arabidopsis halleri* and *A.*
443 *lyrata* (Isaure et al., 2015) or Cd-hyperaccumulator *Noccaea caerulescens* (Küpper et al.,
444 2004), where Cd is associated with glutathione. The possible transportation of Cd as
445 $\text{Cd}(\text{H}_2\text{O})_6^{2+}$ in the xylem sap of *A. halleri* has been proposed by Ueno et al., 2008 (Ueno et
446 al., 2008). In *Brassica napus*, Mendoza-Cózatl et al. (2008) suggested that Cd in xylem
447 sap could also be complexed by oxygen ligands. As for the specific O ligands candidates,
448 histidine has been reported for zinc transport in sap (Küpper et al., 2004), and
449 complexation of Zn by organic acids has been invoked in *A. halleri* xylem sap (Cornu et al.,

450 2015). Given that Cd is considered Zn sister element, and that Sun et al 2006 (Sun et al.,
451 2006) identified increased amount of organic acids in *S. nigrum* when exposed to Cd, we
452 hypothesize that Cd could be transported bound to organic acids in *S. nigrum* xylem sap,
453 though further investigation is needed to rule out the involvement of histidine or
454 $\text{Cd}(\text{H}_2\text{O})_6^{2+}$. As for the phloem, Mendoza-Cózatl (2011, 2008) suggested transport of Cd
455 by non-protein thiol compounds, namely glutathione, and possibly phytochelatins, in
456 *Brassica napus*. This could explain the ligand mixture we measured in *S. nigrum* stem,
457 with Cd being complexed with O ligands in the xylem sap and with S ligands in the phloem
458 sap (Figure 5).

459

460

461 **Storage of S-bound Cd in *S. nigrum* and *S. melongena* leaves.** Our results show that
462 the main first neighbor of Cd in both *S. nigrum* and *S. melongena* fresh leaves is sulfur
463 (Figure 5). In *S. melongena* fresh leaves, 100% of Cd is bound to organic sulfur ligands
464 (glutathione, Figures 4 and 5). In *S. nigrum*, Cd speciation depends on the leaf maturity.
465 Younger, top leaves EXAFS spectrum is best reproduced with three components: Cd
466 bound to organic sulfur (best fit with glutathione, 58.4%), Cd bound to inorganic sulfur
467 (best fit with CdS, 27.1%) and Cd bound to oxygen ligands (best fit: 14.5% -O). While the
468 best LCF fit involves Cd bound to tartrate, the method gives acceptable results for Cd-
469 histidine, $\text{Cd}(\text{H}_2\text{O})_6^{2+}$ and the other organic acids measured. In *S. nigrum*, older, bottom
470 leaves, we found that 100% of Cd is bound to sulfur ligands: 74.4% to organic sulfur
471 ligands (Cd-glutathione) and 25.6% to inorganic sulfur (CdS). For both *S. nigrum* and *S.*
472 *melongena*, our results do not validate Sun et al., 2006 hypothesis that, for plants grown in
473 the same conditions, Cd could be entirely complexed by organic acids in their leaves (Sun
474 et al., 2006), as they reported high amounts of tartrate and acetate in leaves of *S.*
475 *melongena* and of malate in leaves of *S. nigrum*.

476

477 Cd in *S. melongena* leaves.

478 Previous EXAFS studies performed on leaves from Cd-hyperaccumulators *T. praecox*
479 (Vogel-Mikuš et al., 2010) and *Arabidopsis halleri* (Huguet et al., 2012; Isaure et al.,
480 2015) or Cd-tolerant *Arabidopsis halleri* x *A. lyrata* progenies (Isaure et al., 2015) plants
481 demonstrated that Cd is mainly bound to -O ligands, and that S ligands are secondary
482 species. They link complexation of Cd to oxygen ligands to the plant Cd tolerance and its
483 Cd accumulation capacity (Isaure et al., 2015). Interestingly, in non-accumulator
484 *Arabidopsis lyrata* and Cd non-tolerant *Arabidopsis halleri* x *A. lyrata* progenies from
485 Isaure et al. study (Isaure et al., 2015), Cd is coordinated by S atoms only or with a small
486 contribution of O ligands, which is very similar to what we observed in *S. melongena*
487 (100% Cd bound to thiols). As mentioned earlier, Cd chelation by thiol ligands and
488 vacuolar sequestration of these complexes is a known detoxification mechanism in various
489 plants and fungi (Cobbett, 2000; Marentes and Rauser, 2007; Mendoza-Cózatl et al.,
490 2008; Pál et al., 2018; Uraguchi and Fujiwara, 2012; Wawrzyński et al., 2006). Among the
491 non-protein thiol ligands, glutathione is of particular interest. As an antioxidant compound,
492 it plays a major role in the defense against oxidative stress in plants (Cobbett, 2000;
493 Mendoza-Cózatl et al., 2008; Ulrich and Jakob, 2019). Glutathione is also the precursor
494 and building block of phytochelatins (Noctor et al., 2011; Ulrich and Jakob, 2019), which
495 have been identified as Cd chelating agents involved in Cd detoxification mechanisms
496 (Cobbett, 2000; Szalai et al., 2009). Our results point toward a major role of these
497 detoxification mechanisms in *S. melongena*. Genetic and cellular studies show that the
498 vacuolar sequestration of Cd complexed by non-protein thiols are active processes that
499 consume energy to maintain vacuolar to cytoplasmic Cd gradient (Cobbett, 2000; Ulrich
500 and Jakob, 2019). Interestingly, in the dead leaves of *S. melongena*, the amount of Cd
501 bound to thiol ligands dramatically decreases compared to fresh leaves, with values of

502 40% total Cd bound to S ligands (Figures 4 and 5), the remaining Cd being bound to -O
503 ligands (accepted fits with Cd-malate and Cd-tartrate). This is in very good agreement with
504 the existence of an active Cd detoxification mechanism taking place in *S. melongena* fresh
505 tissues.

506

507 Cd in *S. nigrum* leaves.

508 As for *S. melongena*, Cd complexation by thiol ligands plays an important role in *S.*
509 *nigrum*, with values of ~75% in the bottom, more mature leaves. Our results suggest that
510 the remaining Cd in those leaves is bound to inorganic sulfur (Figures 4 and 5). Previous
511 studies reported that Cd may be stored in plants, including *Solanum lycopersicum*, in a
512 stable high molecular complex that incorporate phytochelatins and sulfides (Collin et al.,
513 2014; Pickering et al., 1999; Reese et al., 1992). In fungi, CdS crystallite core coated with
514 phytochelatins were isolated and identified by titration and optical spectroscopy (Bae and
515 Mehra, 1998; Dameron and Winge, 1990). The possibility of a polynuclear Cd cluster with
516 inorganic, bridging sulfides was also suggested by sulfur K-edge EXAFS performed on
517 synthetic Cd-phytochelatin (Pickering et al., 1999). Bae and Mehra proposed that the
518 stability of Cd-phytochelatin complexes is enhanced by the addition of sulfides (Bae and
519 Mehra, 1998). Cadmium detoxification through binding to mineral sulfur has also been
520 observed by Cd K-edge EXAFS spectroscopy, in the bacterium *Stenotrophomonas*
521 *maltophilia* (Pages et al., 2008). We also conclude that the combination of inorganic CdS
522 and Cd bound to thiols compound observed in *S. nigrum* mature leaves constitutes a Cd
523 detoxification mechanism and could explain the enhanced Cd accumulation capacity of *S.*
524 *nigrum* compared to *S. melongena*. In *S. nigrum* younger, top leaves, our results suggest
525 that the same mechanism is involved, as 58% of Cd is bound to thiols and 27% to mineral
526 S. In addition, ~15% of Cd is bound to -O ligands. As the more mature leaves do not show
527 Cd complexation with oxygen ligands, this reinforces our hypothesis that Cd bound to O

528 ligands is a transient form in younger leaves, that could be associated with the
529 translocation and transport of Cd from the roots to the leaves, where Cd would eventually
530 be stored bound to S ligands.

531

532

533

534 **3.4. Environmental implications**

535 Since Cd phytoavailability is tightly linked to its chemical speciation (Cullen and
536 Maldonado, 2013), it is crucial to get direct, experimental access to this parameter. In this
537 context, the developing use of XAS spectroscopy to determine Cd ligands keeps on
538 bringing new information on this metal fate in plants (Huguet et al., 2015; Isaure et al.,
539 2015; Wiggenhauser et al., 2020). We reported here, to our knowledge, the first direct
540 determination of Cd speciation in Solanaceae. We demonstrated that sulfur plays a major
541 role in the detoxification of Cd in these plants, and that oxygen ligands only take part as
542 transport forms for Cd translocation. Our findings do not agree with Sun et al. titration-
543 based hypothesis of a full Cd complexation with organic acids in *S. nigrum* and *S.*
544 *melongena* (Sun et al., 2006), which proves that XAS spectroscopy has a lot to offer to
545 understand Cd distribution in plants. For the first time, a combination of Cd binding to
546 thiolates and to inorganic sulfur was determined in plants, confirming Salt and
547 collaborators intuition in 2002 (Salt et al., 2002). Cao et al. showed that sulfur fertilizer
548 application in rice reduces Cd uptake and translocation to the grains (Cao et al., 2018). In
549 *S. melongena*, a similar result was obtained for chromium: high sulfur supply decreases
550 Cr(VI) toxicity (Singh et al., 2017). As we showed that S is a major agent of Cd
551 detoxification in *S. nigrum* and *S. melongena*, it would be of interest to investigate whether
552 high sulfur supply to these plants may also reduce Cd toxicity.

553

554

555 **Acknowledgments**

556 This work was supported by a MSCA Individual Fellowship (SPECADIS, 794825) awarded
557 to MLP. E. Doelsch has received funding from the EU Horizon 2020 Framework
558 Programme for Research and Innovation under the Marie Skłodowska-Curie actions
559 agreement N°795614. We acknowledge Diamond Light Source for time on Beamline B18
560 under Proposal SP23312. The authors wish to thank D. Gianolo and G. Cibirin for their
561 precious help on the B18 beamline, and A.-K. Geiger for her help in the lab. We
562 acknowledge SOLEIL for provision of synchrotron radiation facilities on Beamline SAMBA
563 under Proposal 20190342, and we would like to thank G. Landrot for assistance in using
564 beamline SAMBA. We thank M.P. Isaure for sharing her Cd references EXAFS spectra,
565 and M. Wiggerhauser for helpful discussions.

566 **References**

- 567 Adeleke, R., Nwangburuka, C., Oboirien, B., 2017. Origins, roles and fate of organic acids in soils: A review. *South*
568 *Afr. J. Bot.* 108, 393–406.
- 569 Bae, W., Mehra, R.K., 1998. Properties of glutathione- and phytochelatin-capped CdS bionanocrystallites. *J. Inorg.*
570 *Biochem.* 69, 33–43. [https://doi.org/10.1016/S0162-0134\(97\)10006-X](https://doi.org/10.1016/S0162-0134(97)10006-X)
- 571 Baize, D., 1997. *Teneurs totales en éléments traces métalliques dans les sols (France)*. INRA Editions, Paris.
- 572 Baker, A., McGrath, S., Reeves, R., Smith, J.A.C., 2000. Metal hyperaccumulator plants: a review of the ecology and
573 physiology of a biological resource for phytoremediation of metal-polluted soils. *Phytoremediation Contamin*
574 *Soil Water* 85.
- 575 Bao, T., Sun, L.-N., Sun, T.-H., 2011a. The effects of Fe deficiency on low molecular weight organic acid exudation
576 and cadmium uptake by *Solanum nigrum* L. *Acta Agric. Scand. Sect. B — Soil Plant Sci.* 61, 305–312.
577 <https://doi.org/10.1080/09064710.2010.493529>
- 578 Bao, T., Sun, T., Sun, L., 2011b. Low molecular weight organic acids in root exudates and cadmium accumulation in
579 cadmium hyperaccumulator *Solanum nigrum* L. and nonhyperaccumulator *Solanum lycopersicum* L. *Afr. J.*
580 *Biotechnol.* 10, 17180–17185.
- 581 Barrow, N.J., Gerth, J., Brümmer, G.W., 1989. Reaction kinetics of the adsorption and desorption of nickel, zinc and
582 cadmium by goethite. II Modelling the extent and rate of reaction. *J. Soil Sci.* 40, 437–450.
- 583 Bruemmer, G.W., Gerth, J., Tiller, K.G., 1988. Reaction kinetics of the adsorption and desorption of nickel, zinc and
584 cadmium by goethite. I. Adsorption and diffusion of metals. *J. Soil Sci.* 39, 37–52.
- 585 Cai, Y., Braids, O.C., American Chemical Society (Eds.), 2003. *Biogeochemistry of environmentally important trace*
586 *elements*, ACS symposium series. American Chemical Society, Washington, DC.
- 587 Cao, Z.-Z., Qin, M.-L., Lin, X.-Y., Zhu, Z.-W., Chen, M.-X., 2018. Sulfur supply reduces cadmium uptake and
588 translocation in rice grains (*Oryza sativa* L.) by enhancing iron plaque formation, cadmium chelation and
589 vacuolar sequestration. *Environ. Pollut.* 238, 76–84.
- 590 Chamseddine, M., Wided, B.A., Guy, H., Marie-Edith, C., Fatma, J., 2008. Cadmium and copper induction of oxidative
591 stress and antioxidative response in tomato (*Solanum lycopersicon*) leaves. *Plant Growth Regul.* 57, 89.
592 <https://doi.org/10.1007/s10725-008-9324-1>
- 593 Chen, Y., Ma, J., Li, Y., Weng, L., 2019. Enhanced cadmium immobilization in saturated media by gradual stabilization
594 of goethite in the presence of humic acid with increasing pH. *Sci. Total Environ.* 648, 358–366.
595 <https://doi.org/10.1016/j.scitotenv.2018.08.086>
- 596 Cobbett, C.S., 2000. Phytochelatins and Their Roles in Heavy Metal Detoxification. *Plant Physiol.* 123, 825.
597 <https://doi.org/10.1104/pp.123.3.825>
- 598 Collin, B., Doelsch, E., Keller, C., Cazevieille, P., Tella, M., Chaurand, P., Panfili, F., Hazemann, J.L., Meunier, J.D.,
599 2014. Copper distribution and speciation in bamboo exposed to a high Cu concentration and Si
600 supplementation. *First Evid. Presence Reduc. Copp. Bound Sulfur Compd. Poaceae Env Pollut* 187, 22–30.
- 601 Cornu, J.-Y., Deinlein, U., Höreth, S., Braun, M., Schmidt, H., Weber, M., Persson, D.P., Husted, S., Schjoerring, J.K.,
602 Clemens, S., 2015. Contrasting effects of nicotianamine synthase knockdown on zinc and nickel tolerance and
603 accumulation in the zinc/cadmium hyperaccumulator *Arabidopsis halleri*. *New Phytol.* 206, 738–750.
604 <https://doi.org/10.1111/nph.13237>
- 605 Cullen, J.T., Maldonado, M.T., 2013. Biogeochemistry of Cadmium and Its Release to the Environment, in: Sigel, A.,
606 Sigel, H., Sigel, R.K. (Eds.), *Cadmium: From Toxicity to Essentiality*. Springer Netherlands, Dordrecht, pp.
607 31–62. https://doi.org/10.1007/978-94-007-5179-8_2
- 608 Dameron, C.T., Winge, D.R., 1990. Characterization of peptide-coated cadmium-sulfide crystallites. *Inorg. Chem.* 29,
609 1343–1348. <https://doi.org/10.1021/ic00332a011>
- 610 Das, P., Samantaray, S., Rout, G.R., 1997. Studies on cadmium toxicity in plants: A review. *Environ. Pollut.* 98, 29–36.
611 [https://doi.org/10.1016/S0269-7491\(97\)00110-3](https://doi.org/10.1016/S0269-7491(97)00110-3)
- 612 Dharma-wardana, M.W.C., 2018. Fertilizer usage and cadmium in soils, crops and food. *Environ. Geochem. Health* 40,
613 2739–2759. <https://doi.org/10.1007/s10653-018-0140-x>
- 614 Doelsch, E., Basile-Doelsch, I., Rose, J., Masion, A., Borschneck, D., Hazemann, J.-L., Saint Macary, H., Bottero, J.-
615 Y., 2006. New combination of EXAFS spectroscopy and density fractionation for the speciation of chromium
616 within an andosol. *Environ. Sci. Technol.* 40, 7602–7608.
- 617 Fan, T.W.-M., Lane, A.N., Pedler, J., Crowley, D., Higashi, R.M., 1997. Comprehensive analysis of organic ligands in
618 whole root exudates using nuclear magnetic resonance and gas chromatography–mass spectrometry. *Anal.*
619 *Biochem.* 251, 57–68.
- 620 Gao, Y., Zhou, P., Mao, L., Shi, W.J., Zhi, Y.E., 2010. Phytoextraction of cadmium and physiological changes in
621 *Solanum nigrum* as a novel cadmium hyperaccumulator. *Russ. J. Plant Physiol.* 57, 501–508.
622 <https://doi.org/10.1134/S1021443710040072>
- 623 Gerth, J., Bruemmer, G., 1983. Adsorption and immobilisation of nickel, zinc and cadmium by goethite (. cap alpha.-
624 FeOOH).

- 625 Gerth, J., Brümmner, G.W., Tiller, K.G., 1993. Retention of Ni, Zn and Cd by Si⁴⁺-associated goethite. *Z. Für*
626 *Pflanzenernähr. Bodenkd.* 156, 123–129.
- 627 Hammer, D., Keller, C., McLaughlin, M.J., Hamon, R.E., 2006. Fixation of metals in soil constituents and potential
628 remobilization by hyperaccumulating and non-hyperaccumulating plants: Results from an isotopic dilution
629 study. *Environ. Pollut.* 143, 407–415. <https://doi.org/10.1016/j.envpol.2005.12.008>
- 630 Han, F., Shan, X., Zhang, S., Wen, B., Owens, G., 2006. Enhanced cadmium accumulation in maize roots—the impact
631 of organic acids. *Plant Soil* 289, 355–368.
- 632 Hasan, Md.K., Ahammed, G.J., Sun, S., Li, M., Yin, H., Zhou, J., 2019. Melatonin Inhibits Cadmium Translocation and
633 Enhances Plant Tolerance by Regulating Sulfur Uptake and Assimilation in *Solanum lycopersicum* L. *J. Agric.*
634 *Food Chem.* 67, 10563–10576. <https://doi.org/10.1021/acs.jafc.9b02404>
- 635 Hasan, Md.K., Ahammed, G.J., Yin, L., Shi, K., Xia, X., Zhou, Y., Yu, J., Zhou, J., 2015. Melatonin mitigates cadmium
636 phytotoxicity through modulation of phytochelatin biosynthesis, vacuolar sequestration, and antioxidant
637 potential in *Solanum lycopersicum* L. *Front. Plant Sci.* 6. <https://doi.org/10.3389/fpls.2015.00601>
- 638 Huguet, S., Bert, V., Laboudigue, A., Barthès, V., Isaure, M.-P., Llorens, I., Schat, H., Sarret, G., 2012. Cd speciation
639 and localization in the hyperaccumulator *Arabidopsis halleri*. *Environ. Exp. Bot.* 82, 54–65.
640 <https://doi.org/10.1016/j.envexpbot.2012.03.011>
- 641 Huguet, S., Isaure, M.-P., Bert, V., Laboudigue, A., Proux, O., Flank, A.-M., Vantelon, D., Sarret, G., 2015. Fate of
642 cadmium in the rhizosphere of *Arabidopsis halleri* grown in a contaminated dredged sediment. *Sci. Total*
643 *Environ.* 536, 468–480.
- 644 Isaure, M.-P., Fayard, B., Sarret, G., Pairis, S., Bourguignon, J., 2006. Localization and chemical forms of cadmium in
645 plant samples by combining analytical electron microscopy and X-ray spectromicroscopy. *Spectrochim. Acta*
646 *Part B At. Spectrosc.* 61, 1242–1252. <https://doi.org/10.1016/j.sab.2006.10.009>
- 647 Isaure, M.-P., Huguet, S., Meyer, C.-L., Castillo-Michel, H., Testemale, D., Vantelon, D., Saumitou-Laprade, P.,
648 Verbruggen, N., Sarret, G., 2015. Evidence of various mechanisms of Cd sequestration in the
649 hyperaccumulator *Arabidopsis halleri*, the non-accumulator *Arabidopsis lyrata*, and their progenies by
650 combined synchrotron-based techniques. *J. Exp. Bot.* 66, 3201–3214. <https://doi.org/10.1093/jxb/erv131>
- 651 Kubier, A., Wilkin, R.T., Pichler, T., 2019. Cadmium in soils and groundwater: A review. *Appl. Geochem.* 108,
652 104388.
- 653 Küpper, H., Mijovilovich, A., Meyer-Klaucke, W., Kroneck, P.M.H., 2004. Tissue- and Age-Dependent Differences in
654 the Complexation of Cadmium and Zinc in the Cadmium/Zinc Hyperaccumulator *Thlaspi caerulescens*
655 (Ganges Ecotype) Revealed by X-Ray Absorption Spectroscopy. *Plant Physiol.* 134, 748–757.
656 <https://doi.org/10.1104/pp.103.032953>
- 657 Landrot, G., 2018. FASTOSH: a software to process XAFS data for geochemical & environmental applications.
658 *Goldschmidt Abstr.* 2018.
- 659 Le Bars, M., Legros, S., Levard, C., Chaurand, P., Tella, M., Rovezzi, M., Browne, P., Rose, J., Doelsch, E., 2018.
660 Drastic Change in Zinc Speciation during Anaerobic Digestion and Composting: Instability of Nanosized Zinc
661 Sulfide. *Environ. Sci. Technol.* 52, 12987–12996. <https://doi.org/10.1021/acs.est.8b02697>
- 662 Li, X., Cui, X., Zhang, X., Liu, W., Cui, Z., 2020. Combined toxicity and detoxification of lead, cadmium and arsenic in
663 *Solanum nigrum* L. *J. Hazard. Mater.* 389, 121874. <https://doi.org/10.1016/j.jhazmat.2019.121874>
- 664 Lin, Z., Schneider, A., Sterckeman, T., Nguyen, C., 2016. Ranking of mechanisms governing the phytoavailability of
665 cadmium in agricultural soils using a mechanistic model. *Plant Soil* 399, 89–107.
- 666 Loganathan, P., Vigneswaran, S., Kandasamy, J., Naidu, R., 2012. Cadmium Sorption and Desorption in Soils: A
667 Review. *Crit. Rev. Environ. Sci. Technol.* 42, 489–533. <https://doi.org/10.1080/10643389.2010.520234>
- 668 Lombi, E., Zhao, F.J., Dunham, S.J., McGrath, S.P., 2000. Cadmium accumulation in populations of *Thlaspi*
669 *caerulescens* and *Thlaspi goesingense*. *New Phytol.* 145, 11–20.
- 670 Lu, L., Tian, S., Yang, X., Peng, H., Li, T., 2013. Improved cadmium uptake and accumulation in the hyperaccumulator
671 *Sedum alfredii*: the impact of citric acid and tartaric acid. *J. Zhejiang Univ. Sci. B* 14, 106–114.
672 <https://doi.org/10.1631/jzus.B1200211>
- 673 Maqbool, A., Rizwan, M., Ali, S., Zia-ur-Rehman, M., 2019. Chapter 12 - Plant Nutrients and Cadmium Stress
674 Tolerance, in: Hasanuzzaman, M., Vara Prasad, M.N., Nahar, K. (Eds.), *Cadmium Tolerance in Plants*.
675 Academic Press, pp. 319–333. <https://doi.org/10.1016/B978-0-12-815794-7.00012-6>
- 676 Marentes, E., Rauser, W.E., 2007. Different proportions of cadmium occur as Cd-binding phytochelatin complexes in
677 plants. *Physiol. Plant.* <https://doi.org/10.1111/j.1399-3054.2007.00960.x>
- 678 Mendoza-Cózatl, D.G., Butko, E., Springer, F., Torpey, J.W., Komives, E.A., Kehr, J., Schroeder, J.I., 2008.
679 Identification of high levels of phytochelatin, glutathione and cadmium in the phloem sap of *Brassica napus*.
680 A role for thiol-peptides in the long-distance transport of cadmium and the effect of cadmium on iron
681 translocation. *Plant J.* 54, 249–259. <https://doi.org/10.1111/j.1365-313X.2008.03410.x>
- 682 Mendoza-Cózatl, D.G., Jobe, T.O., Hauser, F., Schroeder, J.I., 2011. Long-distance transport, vacuolar sequestration,
683 tolerance, and transcriptional responses induced by cadmium and arsenic. *Curr. Opin. Plant Biol.* 14, 554–562.
684 <https://doi.org/10.1016/j.pbi.2011.07.004>
- 685 Nocito, F.F., Lancilli, C., Dendena, B., Lucchini, G., Sacchi, G.A., 2011. Cadmium retention in rice roots is influenced
686 by cadmium availability, chelation and translocation. *Plant Cell Environ.* 34, 994–1008.

- 687 Noctor, G., Queval, G., Mhamdi, A., Chaouch, S., Foyer, C.H., 2011. Glutathione. Arab. Book 9, e0142–e0142.
688 <https://doi.org/10.1199/tab.0142>
- 689 Pages, D., Rose, J., Conrod, S., Cuine, S., Carrier, P., Heulin, T., Achouak, W., 2008. Heavy Metal Tolerance in
690 *Stenotrophomonas maltophilia*. PLoS ONE 3, e1539. <https://doi.org/10.1371/journal.pone.0001539>
- 691 Pál, M., Janda, T., Szalai, G., 2018. Interactions between plant hormones and thiol-related heavy metal chelators. Plant
692 Growth Regul. 85, 173–185. <https://doi.org/10.1007/s10725-018-0391-7>
- 693 Pickering, I.J., Prince, R.C., George, G.N., Rauser, W.E., Wickramasinghe, W.A., Watson, A.A., Dameron, C.T.,
694 Dance, I.G., Fairlie, D.P., Salt, D.E., 1999. X-ray absorption spectroscopy of cadmium phytochelatin and
695 model systems. Biochim. Biophys. Acta BBA - Protein Struct. Mol. Enzymol. 1429, 351–364.
696 [https://doi.org/10.1016/S0167-4838\(98\)00242-8](https://doi.org/10.1016/S0167-4838(98)00242-8)
- 697 Prasad, M.N.V., 1995. Cadmium toxicity and tolerance in vascular plants. Environ. Exp. Bot. 35, 525–545.
698 [https://doi.org/10.1016/0098-8472\(95\)00024-0](https://doi.org/10.1016/0098-8472(95)00024-0)
- 699 Rauser, W.E., 2003. Phytochelatin-based complexes bind various amounts of cadmium in maize seedlings depending
700 on the time of exposure, the concentration of cadmium and the tissue. New Phytol. 158, 269–278.
- 701 Ravel, B., Newville, M., 2005. ATHENA, ARTEMIS, HEPHAESTUS: data analysis for X-ray absorption spectroscopy
702 using IFEFFIT. J. Synchrotron Radiat. 12, 537–541. <https://doi.org/10.1107/S0909049505012719>
- 703 Reese, R.N., White, C.A., Winge, D.R., 1992. Cadmium-Sulfide Crystallites in Cd-(γ EC)_nG Peptide Complexes from
704 Tomato. Plant Physiol. 98, 225. <https://doi.org/10.1104/pp.98.1.225>
- 705 Rehr, J.J., Kas, J.J., Vila, F.D., Prange, M.P., Jorissen, K., 2010. Parameter-free calculations of X-ray spectra with
706 FEFF9. Phys. Chem. Chem. Phys. 12, 5503–5513.
- 707 Rizwan, M., Meunier, J.-D., Miche, H., Keller, C., 2012. Effect of silicon on reducing cadmium toxicity in durum
708 wheat (*Triticum turgidum* L. cv. Claudio W.) grown in a soil with aged contamination. J. Hazard. Mater. 209–
709 210, 326–334. <https://doi.org/10.1016/j.jhazmat.2012.01.033>
- 710 Robson, T.C., Braungardt, C.B., Rieuwert, J., Worsfold, P., 2014. Cadmium contamination of agricultural soils and
711 crops resulting from sphalerite weathering. Environ. Pollut. 184, 283–289.
712 <https://doi.org/10.1016/j.envpol.2013.09.001>
- 713 Salt, D.E., Prince, R.C., Pickering, I.J., 2002. Chemical speciation of accumulated metals in plants: evidence from X-
714 ray absorption spectroscopy. Microchem. J. 71, 255–259.
- 715 Salt, D.E., Prince, R.C., Pickering, I.J., Raskin, I., 1995. Mechanisms of cadmium mobility and accumulation in Indian
716 mustard. Plant Physiol. 109, 1427–1433.
- 717 Samardjieva, K.A., Gonçalves, R.F., Valentão, P., Andrade, P.B., Pissarra, J., Pereira, S., Tavares, F., 2015. Zinc
718 Accumulation and Tolerance in *Solanum nigrum* are Plant Growth Dependent. Int. J. Phytoremediation 17,
719 272–279. <https://doi.org/10.1080/15226514.2014.898018>
- 720 Sarret, G., 2002. Forms of Zinc Accumulated in the Hyperaccumulator *Arabidopsis halleri*. PLANT Physiol. 130,
721 1815–1826. <https://doi.org/10.1104/pp.007799>
- 722 Sarret, G., Smits, E.P., Michel, H.C., Isaure, M.P., Zhao, F.J., Tappero, R., 2013. Use of synchrotron-based techniques
723 to elucidate metal uptake and metabolism in plants, in: Advances in Agronomy. Elsevier, pp. 1–82.
- 724 Singh, M., Kushwaha, B.K., Singh, S., Kumar, V., Singh, V.P., Prasad, S.M., 2017. Sulphur alters chromium (VI)
725 toxicity in *Solanum melongena* seedlings: Role of sulphur assimilation and sulphur-containing antioxidants.
726 Plant Physiol. Biochem. 112, 183–192. <https://doi.org/10.1016/j.plaphy.2016.12.024>
- 727 Sun, R., Zhou, Q., Jin, C., 2006. Cadmium accumulation in relation to organic acids in leaves of *Solanum nigrum* L. as
728 a newly found cadmium hyperaccumulator. Plant Soil 285, 125–134. <https://doi.org/10.1007/s11104-006-0064-6>
- 729
- 730 Sun, R., Zhou, Q., Wei, S., 2011. Cadmium Accumulation in Relation to Organic Acids and Nonprotein Thiols in
731 Leaves of the Recently Found Cd Hyperaccumulator *Rorippa globosa* and the Cd-accumulating Plant *Rorippa*
732 *islandica*. J. Plant Growth Regul. 30, 83–91. <https://doi.org/10.1007/s00344-010-9176-6>
- 733 Szalai, G., Kellös, T., Galiba, G., Kocsy, G., 2009. Glutathione as an Antioxidant and Regulatory Molecule in Plants
734 Under Abiotic Stress Conditions. J. Plant Growth Regul. 28, 66–80. <https://doi.org/10.1007/s00344-008-9075-2>
- 735
- 736 Ueno, D., Iwashita, T., Zhao, F.-J., Ma, J.F., 2008. Characterization of Cd Translocation and Identification of the Cd
737 Form in Xylem Sap of the Cd-Hyperaccumulator *Arabidopsis halleri*. Plant Cell Physiol. 49, 540–548.
738 <https://doi.org/10.1093/pcp/pcn026>
- 739 Ueno, D., Yamaji, N., Kono, I., Huang, C.F., Ando, T., Yano, M., Ma, J.F., 2010. Gene limiting cadmium accumulation
740 in rice. Proc. Natl. Acad. Sci. 107, 16500–16505.
- 741 Ulrich, K., Jakob, U., 2019. The role of thiols in antioxidant systems. Free Radic. Biol. Med. 140, 14–27.
742 <https://doi.org/10.1016/j.freeradbiomed.2019.05.035>
- 743 Uruguchi, S., Fujiwara, T., 2012. Cadmium transport and tolerance in rice: perspectives for reducing grain cadmium
744 accumulation. Rice 5, 5. <https://doi.org/10.1186/1939-8433-5-5>
- 745 Uruguchi, S., Watanabe, I., Yoshitomi, A., Kiyono, M., Kuno, K., 2006. Characteristics of cadmium accumulation and
746 tolerance in novel Cd-accumulating crops, *Avena strigosa* and *Crotalaria juncea*. J. Exp. Bot. 57, 2955–2965.
747 <https://doi.org/10.1093/jxb/erl056>

- 748 Vanderschueren, R., De Mesmaeker, V., Mounicou, S., Isaure, M.-P., Doelsch, E., Montalvo, D., Delcour, J.A., Chavez,
749 E., Smolders, E., 2020. The impact of fermentation on the distribution of cadmium in cacao beans. *Food Res.*
750 *Int.* 127, 108743. <https://doi.org/10.1016/j.foodres.2019.108743>
- 751 Vogel-Mikuš, K., Arčon, I., Kodre, A., 2010. Complexation of cadmium in seeds and vegetative tissues of the cadmium
752 hyperaccumulator *Thlaspi praecox* as studied by X-ray absorption spectroscopy. *Plant Soil* 331, 439–451.
753 <https://doi.org/10.1007/s11104-009-0264-y>
- 754 Vogel-Mikuš, K., Pongrac, P., Kump, P., Nečemer, M., Regvar, M., 2006. Colonisation of a Zn, Cd and Pb
755 hyperaccumulator *Thlaspi praecox* Wulfen with indigenous arbuscular mycorrhizal fungal mixture induces
756 changes in heavy metal and nutrient uptake. *Environ. Pollut.* 139, 362–371.
- 757 Wang, P., Chen, H., Kopittke, P.M., Zhao, F.-J., 2019. Cadmium contamination in agricultural soils of China and the
758 impact on food safety. *Environ. Pollut.* 249, 1038–1048. <https://doi.org/10.1016/j.envpol.2019.03.063>
- 759 Wasserman, S.R., 1997. The analysis of mixtures: Application of principal component analysis to XAS spectra. *J. Phys.*
760 *IV* 7, C2-203-C2-205.
- 761 Wasserman, S.R., Allen, P.G., Shuh, D.K., Bucher, J.J., Edelstein, N.M., 1999. EXAFS and principal component
762 analysis: a new shell game. *J. Synchrotron Radiat.* 6, 284–286.
- 763 Wasylenki, L.E., Swihart, J.W., Romaniello, S.J., 2014. Cadmium isotope fractionation during adsorption to Mn
764 oxyhydroxide at low and high ionic strength. *Geochim. Cosmochim. Acta* 140, 212–226.
- 765 Wawrzyński, A., Kopera, E., Wawrzyńska, A., Kamińska, J., Bal, W., Sirko, A., 2006. Effects of simultaneous
766 expression of heterologous genes involved in phytochelatin biosynthesis on thiol content and cadmium
767 accumulation in tobacco plants. *J. Exp. Bot.* 57, 2173–2182. <https://doi.org/10.1093/jxb/erj176>
- 768 Wei, S.H., Zhou, Q.X., Wang, X., 2005. Cadmium-hyperaccumulator *Solanum nigrum* L. and its accumulating
769 characteristics. *Huan Jing Ke Xue Huanjing Kexue* 26, 167–171.
- 770 Wiggerhauser, M., Aucour, A.-M., Bureau, S., Campillo, S., Telouk, P., Romani, M., Ma, J.F., Landrot, G., Sarret, G.,
771 2020. Cadmium Transfer in Contaminated Soil-Rice Systems: Insights from Solid-State Speciation analysis
772 and Stable Isotope Fractionation. *Environ. Pollut.* 115934. <https://doi.org/10.1016/j.envpol.2020.115934>
- 773 Zhai, L., Liao, X., Chen, T., Yan, X., Xie, H., Wu, B., Wang, L., 2008. Regional assessment of cadmium pollution in
774 agricultural lands and the potential health risk related to intensive mining activities: A case study in Chenzhou
775 City, China. *J. Environ. Sci.* 20, 696–703. [https://doi.org/10.1016/S1001-0742\(08\)62115-4](https://doi.org/10.1016/S1001-0742(08)62115-4)
- 776 Zhou, Q.X., Song, Y.F., 2004. Principles and methods of contaminated soil remediation. *Sci. Beijing Chin.*
777

778

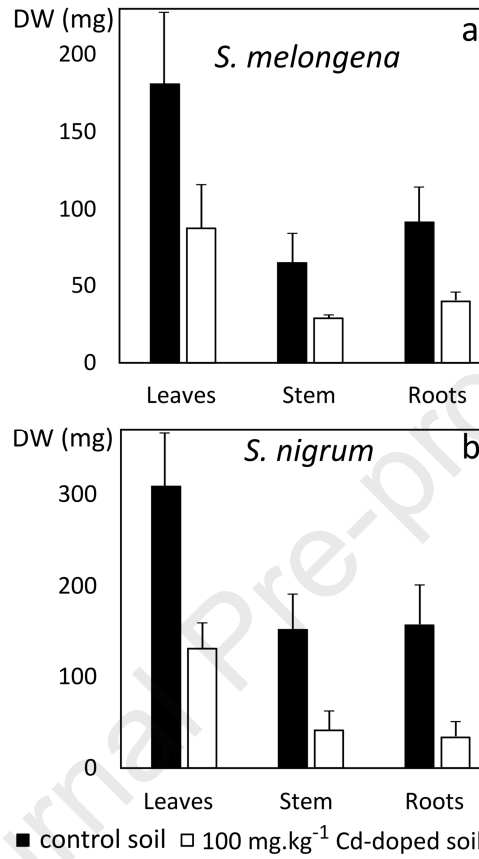
779 **Figures**

780

781

782

783



784

785

786

787

788

Fig. 1. Dry weight (DW) in milligrams of plant parts from *S. melongena* (a) and *S. nigrum* (b) grown on 100 mg.kg⁻¹ Cd-doped soil and control soil. Error bars are 1 s.d.

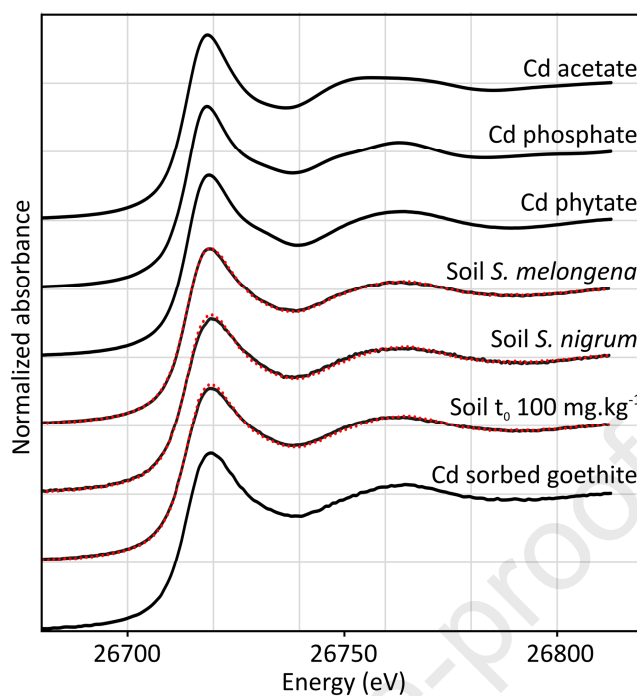
789
790791
792
793
794
795
796
797
798
799
800
801
802

Fig. 2. Cd K-edge XANES spectra of 100 mg.kg⁻¹ Cd-doped pre-culture soil (Soil t₀) and post-culture soils (Soil *S. melongena* and Soil *S. nigrum*; solid dark grey lines) and their respective reconstructed best fits (LCF; dotted red lines). LCF parameters are given in Supplementary Table S9. Cd K-edge XANES spectra of some relevant Cd reference compounds for comparison (Cd sorbed goethite, Cd-phytate, Cd-phosphate and Cd-acetate).

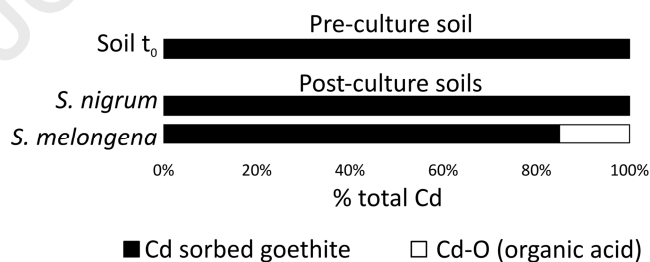
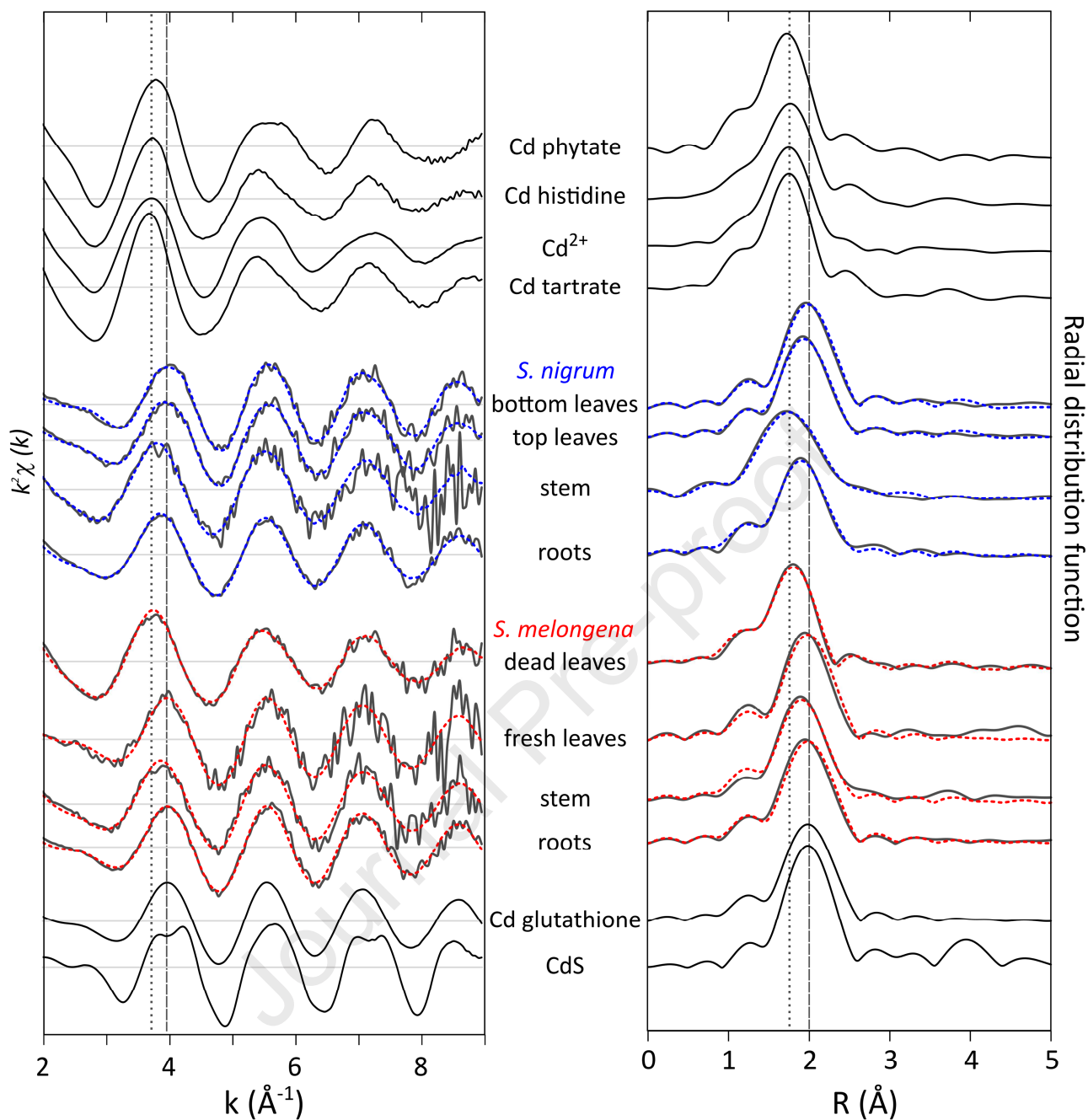
803
804

Fig. 3. Proportion of Cd species (in % mole fraction) in pre- and post-culture soils treated with 100 mg.kg⁻¹ Cd, obtained by XANES linear combination fitting. The percentages were normalized to 100%. The uncertainty of each compound proportion was estimated to $\pm 15\%$. LCF parameters are given in Supplementary Table S9.



805

Fig. 4. Cd K-edge EXAFS spectra (left) and Fourier transforms (FT, radial distribution function – uncorrected for phase shift functions; right) giving the radial distances of the nearest neighbors to Cd for plant parts of *S. nigrum* and *S. melongena* (dark grey solid lines) after 14 weeks of Cd exposure on a 100 mg.kg^{-1} Cd-doped soil. Red dotted lines: reconstructed best fits (LCF) for *S. melongena* EXAFS spectra and associated FT. Blue dotted lines: reconstructed best fits (LCF) for *S. nigrum* EXAFS spectra and associated FT. LCF parameters are given in Supplementary Table S11. Black solid lines: EXAFS spectra and FT of some relevant Cd reference compounds for comparison. Vertical dotted lines: distance R or wave-number k associated with Cd bound to O atoms in its first shell. Vertical dashed lines: distance R or wave-number k associated with Cd bound to S atoms in its first shell.

806

807

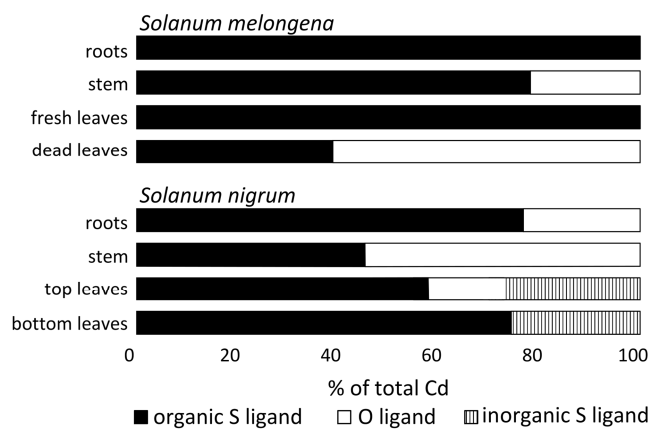


Fig. 5. Proportion of Cd species (in % mole fraction) in *S. melongena* and *S. nigrum* plant parts (plants grown on a 100 mg.kg^{-1} Cd-doped soil) obtained by EXAFS linear combination fitting. The percentages were normalized to 100%. The uncertainty of each compound proportion was estimated to $\pm 15\%$. LCF parameters are given in Supplementary Table S11.

808
809
810
811

Highlights

- X-ray absorption Cd speciation in *Solanum nigrum* and *S. melongena* was reported.
- Cd in the pre- and post-culture clayey loam soils was bound to iron oxyhydroxides.
- In *S. melongena* roots and fresh leaves, Cd was fully bound to thiol ligands.
- In *S. nigrum* leaves, Cd detoxification involved binding to thiols and inorganic S.
- In both plants, Cd transportation involved partial complexation with organic acids.

Declaration of interests

The authors declare that they have no known competing financial interests or personal relationships that could have appeared to influence the work reported in this paper.

The authors declare the following financial interests/personal relationships which may be considered as potential competing interests:

Journal Pre-proof